

Analytical Methods

Accepted Manuscript



This is an *Accepted Manuscript*, which has been through the Royal Society of Chemistry peer review process and has been accepted for publication.

Accepted Manuscripts are published online shortly after acceptance, before technical editing, formatting and proof reading. Using this free service, authors can make their results available to the community, in citable form, before we publish the edited article. We will replace this *Accepted Manuscript* with the edited and formatted *Advance Article* as soon as it is available.

You can find more information about *Accepted Manuscripts* in the [Information for Authors](#).

Please note that technical editing may introduce minor changes to the text and/or graphics, which may alter content. The journal's standard [Terms & Conditions](#) and the [Ethical guidelines](#) still apply. In no event shall the Royal Society of Chemistry be held responsible for any errors or omissions in this *Accepted Manuscript* or any consequences arising from the use of any information it contains.

ARTICLE

Continuous Flow Microfluidic Solution for Quantitative Analysis of Active Pharmaceutical Ingredient Content and Kinetic Release

D. Desai^a and M. H. Zaman^{a,*}

Received Oct 7, 2014.

Accepted 00th January 2XXX

DOI: 10.1039/x0xx00000x

www.rsc.org/

Counterfeit and substandard medicines are a grave public health concern that comprises a multibillion-dollar black market and claims over 100,000 lives every year. The World Health Organization estimates that 1-50% of medicines in countries around the world are adulterated, and their presence imposes serious financial and economic burdens while also contributing to the rise of drug-resistant pathogens. Although there are a number of technologies available for field-based quality screening, none can reliably quantify active pharmaceutical ingredient (API) content or kinetic release from a dissolving tablet at the point of care. This work presents an alternative analytical technique to address this major gap. Our system can specifically and accurately quantify drug API content and kinetic release using a portable, inexpensive, and easy-to-use aptamer based fluorescence platform. We demonstrate that aptamers can provide a simple and effective way to target a wide range of APIs, while maintaining high quantitative precision and accuracy. A microfluidic, flow-through system is employed to obtain drug quality information using a single step procedure that shows an accuracy of over 97% for both API quantification and kinetic release.

Introduction

As we continue to celebrate decades of advancements in modern medicine, millions of sick around the world find themselves amidst a realm of failed treatments. In recent years, substandard and counterfeit medicines have claimed the lives of close to 1M people around the globe and have crushed successful treatment plans for millions more.¹ In countries such as Nigeria and Pakistan, over 40% of the medicines market is composed of adulterated medication,^{1,2} and globally, the World Health Organization (WHO) reports numbers ranging anywhere from 1-50%.^{3,4} Many reports indicate a difficulty in precisely defining the scale of the problem, but what is absolutely certain is that it is staggeringly higher than it ought to be.⁵⁻⁷ The counterfeit drug market is estimated to be worth upwards of \$75B, and the numbers are only rising.⁸

In light of the growing problem, numerous technologies have been used to address this issue.⁹⁻¹⁶ The Global Pharma Health Fund (GPHF) MiniLab[®] system is one example that utilizes thin layer chromatography to quickly separate tablet ingredients and identify them colorimetrically. It currently serves as the gold standard in the field and is used in over 65 countries across the world.¹⁷ However, in spite of its far reach and inexpensive nature, MiniLab[®] only provides a cursory screening for medicines quality, passing tablets that contain as little as 80% of the intended API dosage while the WHO stipulates this number to be between 90-110%.^{18,19} Further work conducted by Weaver *et al.* increases test specificity and selectivity using paper chromatography by adding additional sample lanes and targeting detection of known API

substitutes;²⁰ however, quantitative precision remains an important and persistent problem among these techniques. Colorimetric chromatography approaches also suffer from similar separations for chemicals of varying structure,²¹ or similar color responses for true APIs compared to other analytes.²² Overall, low-cost, separation-based techniques provide excellent accessibility and cursory analysis, but set a low standard for quality testing, decreasing field-based decision making power and increasing the number of tablets that must be sent to slow and cumbersome central facilities for more rigorous testing. They also provide no information regarding API kinetic release, an important quality control factor for tablet formulations.

The emergence of handheld spectroscopic technologies based on near-infrared (NIR) and Raman have provided the opportunity for more rigorous testing while still operating in the field. These methodologies have the additional advantage of being non-destructive, testing tablet quality through packaging. However, these features lead to a new set of challenges. NIR technologies such as Phazir[™] fall victim to problems such as poor sample penetration and sensitivity to light, humidity, and sample position.¹⁹ Raman technologies such as TruScan overcome these, but are still highly sensitive to fluorescent molecules, which are common among APIs.^{10,19} Furthermore, these spectroscopic methods require extensive training sets and reference libraries in order to analyze the spectral fingerprints of their samples for proper tablet formulation and APIs. In addition to complicating calibration, this also leaves them sensitive to innocuous batch-to-batch variations in authentically manufactured tablets. Moreover, while the spectral information

1 can be used to collect quantitative information regarding API
2 content, it cannot be done reliably and still cannot be used to
3 determine API kinetic release.

4 In recent years, the growth and synergistic use of these
5 technologies has led to a notable impact on the spread and
6 prevalence of adulterated medicines. However, another hurdle
7 preventing further progress has been the disproportionate focus
8 that has been put on *counterfeits* drugs. These are broadly
9 defined as imitations sold with the intent to deceive.³ There is
10 now mounting evidence that suggests that beyond these knock-
11 offs, *substandard* medicines are a considerably larger
12 problem.^{23, 24} These medicines are intended for therapeutic use
13 but contain an inappropriate quantity of API and generally do
14 not meet manufacturing requirements. In addition to providing
15 poor treatment, the use of substandard medicines is linked with
16 a secondary and potentially devastating outcome—the
17 cultivation of drug resistant pathogens.²⁴⁻²⁷

18 Substandard medicines present a complex challenge for
19 medicines regulatory authorities around the world, and while
20 existing quality screening tools are well suited to identify
21 counterfeits, substandards can only be reliably addressed
22 through quantitative analysis of API content and kinetic release.
23 Analyzing these attributes ensures not only that the correct API
24 dosage is present, but also that the tablet itself is correctly
25 formulated to deliver the API as intended. These qualities
26 represent a critical need that remains to be adequately
27 addressed by currently available field-based technology. No
28 existing field technology is capable of reliable API
29 quantification and kinetic release analysis. While, trade-offs
30 between quantitative ability and field-readiness are a common
31 struggle, a strategic, systems-level approach that designs
32 around these constraints can be used to overcome this challenge
33 and deliver a technology that can address this gap to detect
34 substandard medicines without sacrificing quantitation or field-
35 readiness. In this work, we pursue this holistic approach to
36 design a platform that lays the foundation and provides promise
37 for such a technology.

38 Experimental

39 Platform Design

40 All field-based devices share common design challenges. In
41 order to be successful, they must be lightweight, low-cost, and
42 capable of operating in a wide range of environmental
43 conditions. Additionally, existing field technologies in
44 medicines screening exhibit numerous pitfalls including
45 inadequate API specificity for quantitation and the use of an
46 endpoint assay that provides only a single snapshot of API
47 content. For the development of a new field-based screening
48 tool, all of these factors must steer the course for fundamental
49 technology considerations that help achieve two major
50 functional objectives: API quantification and API kinetic
51 release. Aligning these multi-faceted factors led to a
52 microfluidic, flow-through design that utilizes fluorescent
53 reporters or tags to specifically quantify dissolving API
54 molecules from a tablet in solution (**Figure 1**). Microfluidics
55 has consistently proven to decrease resource consumption,
56 reducing cost and weight, and furthermore enables controlled
57 analytical testing that can be isolated from environmental
58 conditions. Meanwhile, a flow-through design enables
59 continuous monitoring of API content from a dissolving tablet,
60 expanding existing end-point approaches to a more analytical
time-based test. The use of fluorescent reporters also enables a
tunable method for targeted API quantification and modularizes

the platform by decoupling specificity and sensitivity from the
testing approach itself. This strategy allows for constant
improvements to assay performance through the development
of more specific, brighter reporters without any changes to the
overall system architecture or hardware. These design
considerations combine to produce a platform that is targeted
for field-based screening without sacrificing analytical rigor.

Chip design

The microfluidic chip itself provides a miniaturized testing
space through which small samples of the dissolving tablet
solution can be continuously monitored for API content. This
monitoring occurs through the use of a fluorescent reporter
solution that is specific to the API of interest and mixes
together with the tablet solution on-chip. On-chip mixing
avoids combining a larger reporter volume with the dissolving
tablet solution itself, and furthermore mitigates any effects the
reporter may have on the kinetic release of the API. Microfluidic
mixing strategies have multiplied over the years,
ranging from fluid injectors²⁸ to lamination schemes²⁹⁻³⁴ to
chaotic advection chips.³⁵⁻⁴² However, many of these designs
require complex fabrication procedures. For our application, we
utilized a simple staggered-herringbone (SHM) design reported
by Stroock *et al* and demonstrated to produce efficient mixing.
^{43, 44} While, several groups have further enhanced fluid
advection through additional patterned surfaces,^{45, 46} these
designs again require ancillary fabrication steps that add to
overall chip complexity. **Figure 2** provides a schematic of the
SHM design and demonstrates how fluorescence readings taken
just upstream of the chip egress can be used to determine the
API concentration within the flow-through. Channel
dimensions were chosen to maintain constant fluid velocity
throughout the chip.

Key Fluorescent Reporter Attributes

To successfully quantify an API with high specificity and
sensitivity, the fluorescent reporters must exhibit two key
qualities. The first is good binding, characterized by both a low
dissociation constant, k_d , and fast rate of binding, k_{on} . For a
simple binding system

$$k_d = \frac{[R][L]}{[RL]},$$

where $[R]$ is the concentration of free reporter, $[L]$ is the
concentration of free ligand or API, and $[RL]$ is the
concentration of the bound species. In this case, k_d represents
the concentration of free reporter at which 50% of all API
molecules will be bound. The k_d can also be expressed as the
ratio of the rates of dissociation and association of the bound
complex, expressed as

$$k_d = \frac{k_{off}}{k_{on}}.$$

With our approach focusing on the quantification of
micromolar concentrations, k_d values in the range of 10^{-9} M or
lower ensures that binding to the API occurs to completion.
Fast binding kinetics, or a high k_{on} , is also necessary in order to
ensure that this binding saturation occurs before the fluid
mixture exits the chip. Satisfying these conditions ensure that
the rate of dissociation, k_{off} , falls within a sufficient range to
accurately quantify API concentration while the fluid mixture
remains on-chip. The second key attribute for the fluorescent

reporters is a significant change in the fluorescence signature upon binding. While this includes shifts in either the excitation

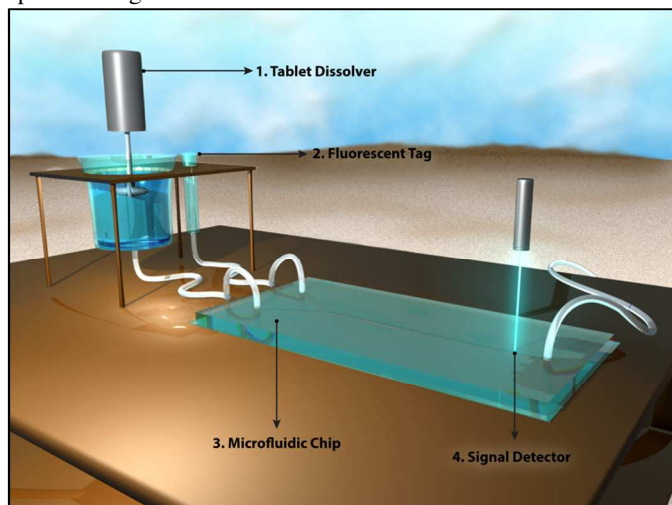


Figure 1 Conceptualization of the substandard medicines screening platform, containing four major components. A pill is dissolved in the tablet dissolver and samples are continuously pumped into the microfluidic chip, along with the fluorescent reporter. These liquids mix on the chip, and a fluorescence reading from the tag is used to determine tablet API content and plot API release over time.

or emission wavelengths, we focus on reporters that show a marked change in fluorescence intensity. From a device design perspective, this limits the number of light sources and filters required for fluorescence detection. The change in fluorescence intensity can then be used to create a standard curve for fluorescent signal as a function of API concentration.

These two key attributes provide a simple mechanism by which API concentration can be continuously monitored to provide a concentration curve as a function of time that reflects the rate at which the API is released from a dissolving tablet. This curve can then be integrated to quantify total API content, providing both quality attributes from a single procedure.

Testing Approach

In order to test the quantitative capacity of our microfluidic, fluorescence-based design, dynamic analyte solutions were created and analyzed using the microfluidic chip. We use the term *dynamic analyte solution* to refer to one in which the target analyte concentration continuously changes over time, simulating a dissolving tablet. We demonstrate the quantitative power of our method by first showing API quantification and kinetic analysis of a model analyte followed by similar results using a real API. Both sets of results were also compared to an analytical model that provided a mathematical basis for the expected outcomes.

Tests conducted with the model system involved the use of streptavidin as an API substitute and biotin-4-fluorescein (B4F) as the fluorescent reporter. The streptavidin-biotin binding pair has been widely used in the biological sciences due to both its high bond strength and fast binding kinetics,^{47, 48} and B4F has also been found to be specifically quenched upon binding to streptavidin.^{49, 50} Prior work conducted by Kada *et al.* demonstrated that B4F was quenched by approximately 88% when bound to a pocket on streptavidin⁵¹, but found that the quenching was dependent on the binding stoichiometry. Due to the four biotin-binding sites available on each streptavidin molecule, ratios of B4F to streptavidin of less than 4:1 resulted

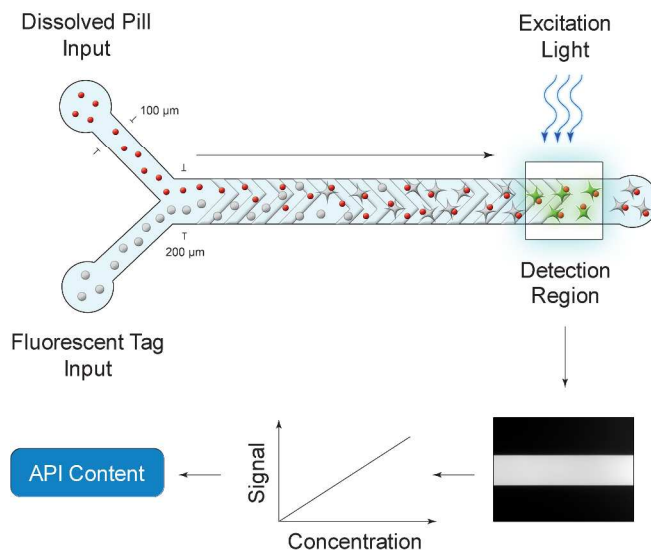


Figure 2 Schematic of the microfluidic chip, with dissolved pill and probe inputs, mixing chamber, and the detection region from which fluorescence readings are compared to a standard curve to determine API concentration.

in a nonlinear fluorescence curve. However, for ratios greater than 4, a sharp and linear rise in fluorescence intensity for increasing concentrations of B4F was observed. This indicated that as long as the number of biotin-binding sites was saturated on each streptavidin molecule, a linear response curve for B4F fluorescence could be used to quantify streptavidin concentration. Indeed, this has been demonstrated in the literature.⁵² These qualities satisfy both attributes outlined for a good fluorescent reporter, with the linear change in B4F fluorescence intensity allowing for analytical detection of streptavidin. To help corroborate our findings for streptavidin quantification using B4F, a method control was performed using the Pierce[®] BCA protein assay to independently quantify streptavidin concentration.

Once validated using a model system, our microfluidic approach was tested on a real API. Tetracycline, an antibiotic, was quantified using the well-studied tetracycline aptamer. According to the literature, binding of tetracycline to this aptamer results in enhancement of tetracycline autofluorescence by several orders of magnitude and occurs with fast binding kinetics.⁵³⁻⁵⁵ These qualities again satisfy the two key attributes for a good fluorescent reporter, allowing the use of the tetracycline aptamer as a means to monitor and quantify tetracycline concentration.

Materials and Methods

Chip fabrication and interfacing. Microfluidics chips were fabricated using polydimethylsiloxane (PDMS) cast on an SU8 mold. The molds were made using two spin-coat layers consisting of SU8-2025 (2600 rpm) followed by SU8-2010 (1200 rpm). Each layer was exposed to a 350 nm light source through a chromium photo mask using the Süss MicroTec MA6 mask aligner. The mold was developed using SU8 developer after both layers had been spun. PDMS was mixed using the Sylgard 184 silicone elastomer kit at a 10:1 ratio and cured at 150°C for 10 min. Chip ports were cored using a 1.0 mm core (Fisher Scientific, 50-309-49) and individual cored chips were

1 bonded to glass slides after O₂ plasma exposure using the PVA
2 TePla M4L plasma asher. All chips were flushed with
3 deionized water for 5 min just before use. Tubes of 1.09 mm
4 OD (Fisher Scientific, NC9152011) were used to interface with
5 the PDMS chips by inserting them directly into the chip ports.
6 The inlet tubes were coupled to larger 1.02 mm ID tubes (Cole-
7 Parmer, EW-95607-28) using union connectors (Cole-Parmer,
8 EW-06473-00), and these larger tubes were loaded onto an 8-
9 channel Ismatec peristaltic pump. (Cole-Parmer, FF-7802312).
10 This pump and interface was used for all subsequent studies.

11 **Dynamic analyte solution preparation.** The dynamic analyte
12 solutions for all kinetic analysis experiments were created by
13 titrating a concentrated 2 ml analyte volume into a larger 30 ml
14 dilution volume of deionized water using the peristaltic pump
15 operating at 10% power. This power setting resulted in an
16 observed flow rate of 130 µl/min, leading to a titration time of
17 ~15 min.

18 **Kinetic analysis analytical model.** An analytical model to
19 describe the kinetic analysis experiments was also used to
20 determine the theoretical concentration profiles expected under
21 the experimental conditions. The assumptions for the model
22 were that the titrant flow rate going into the dilution volume for
23 the dynamic analyte solution was equal to the sampling rate
24 from the mixture. This allowed for a constant volume
25 approximation for the dilution volume, resulting in the
26 description,

$$\frac{dC(t)}{dt} + \frac{Q}{V}C(t) = \frac{Q}{V}C_s,$$

27 where $C(t)$ is the analyte concentration in the dilution volume,
28 Q is the volumetric flow rate, V is the volume of the dynamic
29 analyte solution, and C_s is the concentration of the titrant. The
30 solution to this equation is,

$$C(t) = \begin{cases} c_s \left(1 - e^{-\frac{Q}{V}t}\right), & t < t_e, \\ C(t_e), & t \geq t_e \end{cases}$$

31 where t_e signifies the time at the end of titration. The initial
32 condition used to arrive to this solution was $C(0) = 0$.

33 **Streptavidin-B4F standard curve.** A B4F standard curve was
34 determined to relate B4F fluorescence intensity to streptavidin
35 concentration. Four 1 ml solutions of streptavidin were
36 prepared with concentrations of 1-4 µM. An 8 ml working
37 solution of 18 µM B4F was prepared using the stock solution.
38 The 18 µM concentration was chosen to ensure saturation of
39 biotin binding pockets at the maximum streptavidin
40 concentration of 4 µM according to the stoichiometry of the
41 binding. Each streptavidin sample was successively pumped
42 through the microfluidic chip with the B4F solution using 2
43 channels of the peristaltic pump operating at 10% power.
44 Fluorescence images were taken using a Leica confocal
45 microscope with fluorescein filter cubes at a rate of 2 Hz for 1.5
46 min per sample. A 488 nm laser set to 44.9 mW was used as an
47 excitation source, and images were captured using a 400 ms
48 exposure and 4x4 binning.

49 **Standard curve signal processing.** Fluorescence signals of the
50 standard curve samples measured from time-lapsed images
51 were filtered using Matlab to remove cyclic peaks and valleys
52 in the fluorescence intensity caused by out-of-phase pulsatile

flow of the two solutions from the peristaltic pump. These
peaks were identified and analyzed for the average peak
separation, d_p , in units of images; $10d_p$ was used as the basis of
a windowing algorithm used to analyze local mean values over
the full image set. These averages were used to discard local
outliers beyond a 25% threshold between the mean and the
extreme values of the data range. Once these outliers were
removed, the surviving data was then further analyzed to
identify data clusters within each pulsatile oscillation. These
clusters represented the true fluorescence signal for the sample
during steady flow, while the remaining data were snapshots of
the signal departing from or returning to the steady-state
fluorescence value. The data clusters were isolated by
measuring the average distance between points and eliminating
those whose distance lay outside of ½ standard deviations from
the mean. These thresholds were chosen empirically. Mean
values from within each pump cycle of the remaining data was
then averaged to yield the overall mean fluorescence signal for
the given sample concentration.

53 **Streptavidin-biotin kinetic analysis.** The same 8 ml B4F
54 solution from the standard curve experiment was used to
55 perform this study. During the experiment, streptavidin stock
56 was used to create a dynamic streptavidin solution from which
57 continuous samples were drawn and pushed through the
58 microfluidic chip using the same pump and power settings. A
59 second pumping channel was used to also deliver the 18 µM
60 B4F solution to the chip. Fluorescence readings were recorded
at a rate of 2 Hz for 60 min using the same microscope and
capture settings as for the standard curve. While the titration
time was estimated to take 20 min, data was collected over 1 hr
to observe any deviations from the expected plateau once the
titrant had been depleted. Images were again processed to filter
out artifacts due to pulsatile flow.

Kinetic analysis signal processing. As time-lapsed images of a
dissolution curve are not expected to yield a constant signal
over time, a modified approach was taken to filter out the
pulsatile flow artifacts. As before, a window-based approach
was taken to remove large outliers from the data. Next, data
clusters were again identified, but this time through the use of a
density map. Regions of data were discarded where the density
was outside a ½ standard deviation of the local mean density.
Subsequent to the processing, a linear decrease in signal over
the plateau region due to stage drift was observed for each
experiment and was corrected by adding a constant, linear
correction factor to the full dataset.

BCA kinetic analysis. An identical experimental setup to the
streptavidin quantification study was used to collect
fractionated samples from the microfluidic chip outflow. Each
sample was collected for 1 min for the first 40 min, and for 1.5
min thereafter. The samples were plated on a 96-well plate,
along with streptavidin standard curve samples. The standard
Thermo Scientific™ Pierce™ BCA Protein Assay protocol was
used for analysis, with the exception of performing an 80 min
incubation at 37°C followed by an overnight incubation at 4°C.

Tetracycline aptamer preparation. The aptamer sequence
provided in a Promega SP6/T7 plasmid vector was used to
transform competent *E. coli* cells. Plasmids were amplified and
extracted from 4 ml tube cultures using a Qiagen miniprep kit
(Qiagen, 12125). These plasmids were then linearized using a
standard *HindIII* digest (NEB, R3104T) and transcribed *in vitro*

using T7 polymerase (NEB, M0251L) and a ribonucleotide mix (NEB, N0466L). The RNA product was isolated with an ethanol precipitation, resuspended in UltraPure water (Invitrogen, 10977015) and stored at 4°C until use.

Tetracycline aptamer fluorescence studies. According to the literature, binding of tetracycline to the aptamer results in enhancement of tetracycline autofluorescence by 2-3 orders of magnitude. To verify this behavior, a fluorescence study was performed using a spectrophotometer. The fluorescence intensity of tetracycline-aptamer complex was observed along with controls of solutions including a blank, tetracycline only, and aptamer only. The tetracycline solution was prepared at a concentration of 10 μM , and the aptamer solution was prepared at 6.4 μM , ensuring saturation of bound aptamer. A second study was performed using the same aptamer solution, but with tetracycline concentrations ranging from 0-10 μM . This provided an indication of tetracycline-aptamer stoichiometry, with the expectation of a saturated signal above 6 μM of tetracycline.

Tetracycline standard curve. A 100 μM working solution of tetracycline was prepared from the stock and used to create 4 samples of concentrations from 1-4 μM . A 10 ml aptamer solution of 7.16 μM was also prepared as the probe solution, where a concentration of just under double the maximum tetracycline concentration ensured saturation of tetracycline binding. Samples were pumped through the microfluidic chip with the probe solution, and images were taken using a fluorescence microscope with DAPI filter cubes, but no emission filter (appropriate filter cube was not available). Images for each sample were taken for 1.5 min at 2 Hz using a 250 ms exposure and 8x8 binning. The resulting data was averaged without signal processing, as spikes in fluorescence were not as pronounced as in the streptavidin studies.

Tetracycline kinetic analysis. A 48.64 μM tetracycline solution was prepared to approximately match the streptavidin stock solution concentration. The same procedure as the streptavidin quantification study was performed, but using this tetracycline solution and the same aptamer solution from the tetracycline standard curve study. Images were taken with the fluorescence microscope for ~35 min to provide ample data collection in the plateau region of the concentration curve. Images were processed to remove artifacts due to pulsatile flow. Changes in dissolution apparatus and probe volumes over the course of the experiment were used to correct for any deviations from 1:1 on-chip mixing.

Results

Streptavidin-B4F studies

An on-chip streptavidin-B4F standard curve was obtained to determine a relationship between B4F fluorescence intensity and streptavidin concentration (Figure 3). The standard curve demonstrated a perfect linear trend with low variance and an R^2 value of 0.99. However, the raw data collected to construct the curve showed sharp temporal fluctuations in fluorescence signal over the capture time and was processed to extract relevant data points (Supplemental 1). These fluctuations were cyclic and attributed to the pulsatile nature of the peristaltic pump. While data processing removed much of the large signal fluctuations from the raw data, a periodic pattern was still observed after processing. To avoid these misrepresentative

variations in the final analysis, the mean signal during each cycle was calculated, and the grand mean was used as the final fluorescence reading for each streptavidin concentration. The error bar for each point on the standard curve thus reflects the standard deviation for the grand mean of each data set. While data processing caused an overall decrease in sample size compared to the raw data, it still provided over 60 fluorescence readings for concentration. This provided high statistical confidence for each point of the standard curve in spite of the large signal fluctuations observed in the raw data.

The B4F standard curve was next used to interpret data from the streptavidin kinetic analysis study. The raw data, provided in Figure 4, demonstrates the need for further signal processing to remove artifacts of pulsatile flow. The artifacts manifest as sharp and cyclic fluctuations in signal caused by pulsatile flow in the system. In spite of these fluctuations in fluorescence, a discernable trend is clearly visible in the plot, where an initial rise in signal is observed as the reagents reach the microfluidic chip, followed by a steady decrease caused by quenching due to increasing streptavidin concentration. The minor rise in the plateau region was also subtracted from the full data set before using the standard curve to obtain a concentration profile. The final concentration curve is presented in Figure 5, where the data is also compared to an independent protein quantification assay as well as the analytical model. The plot demonstrates very close agreement of the data from all three approaches. We found only a 2.0% difference in the concentration rate of increase between our approach (245.3 nM/min) and the BCA assay (250.3 nM/min), and a low error of 2.5% from the theoretical value (251.5 nM/min). Integration of the signal yielded a total streptavidin content of 5.13 mg compared to an actual value of 5.0 mg, representing a 2.6% error. In spite of the pulsatile flow and stage drift challenges, the data demonstrates that we were able to not only accurately monitor analyte concentration in a dynamic solution, but also accurately determine total analyte content. We were also able to do this with higher precision than the BCA assay, which shows considerably more variability in the plateau region of the curve.

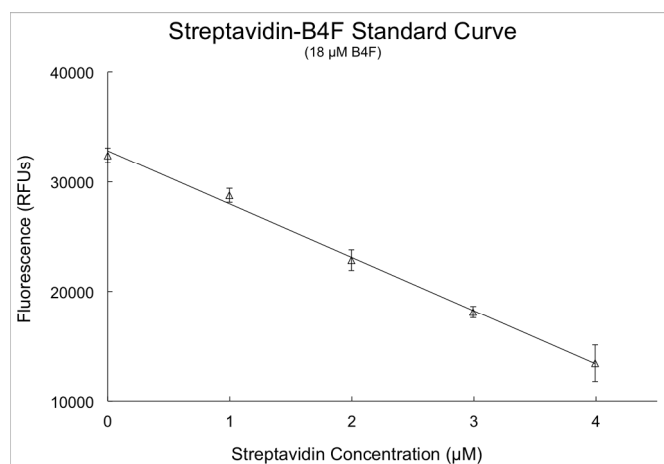


Figure 3 Streptavidin-B4F standard curve for a single run obtained on-chip using 18 μM B4F. This concentration was used to ensure saturation of all four biotin binding sites on each streptavidin molecule so as to avoid confounding data that would otherwise arise from differential quenching from streptavidin molecules with different numbers of bound ligand. Data for each point was collected and averaged over 90 s. Error bars represent the standard deviation of the mean signal

observed for each pulse of the peristaltic pump. The coefficient of determination was 0.99.

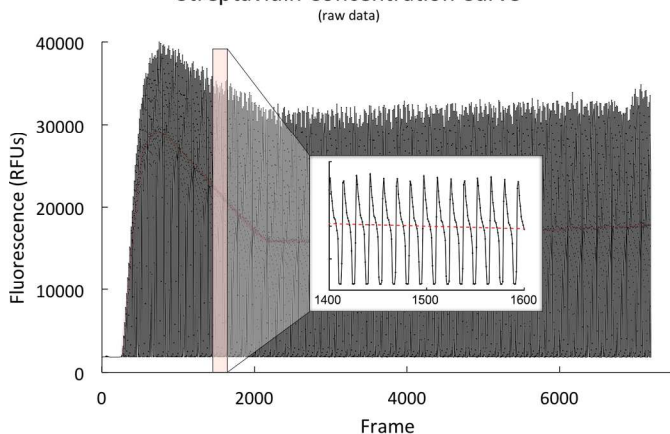


Figure 4 Plot of raw streptavidin concentration curve consisting of fluorescence intensity plotted against image frame. Graph shows periodic fluorescence peaks and valleys that are artifacts of the pulsatile flow generated by the peristaltic pump. A closer look at the central region of the data reveals a higher density data set that represents the true fluorescence reading between cycles of the peristaltic pump. The figure inset provides a closer look at the oscillating data, and highlights the central region represented the true fluorescence signal.

Tetracycline studies

By verifying the quantitative capability of our approach with the streptavidin studies, the next focus was demonstrating that the approach could be used to quantify tetracycline, a small molecule antibiotic. Studies verifying the behavior of the tetracycline aptamer demonstrated that enhanced tetracycline fluorescence was only observed when both tetracycline and the aptamer were present in the same solution (**Figure 6** inset). The data confirmed that virtually no fluorescence was detected in either a blank, tetracycline-only, or aptamer-only solution. In contrast, the solution with both the tetracycline and the aptamer showed over a 90-fold increase in signal. The subsequent stoichiometry study, presented in the plot in **Figure 6**, qualitatively confirmed a 1:1 ratio, showing a plateau in the fluorescence signal at approximately 6 μM of tetracycline. However, the linear range in the plot was observed from 0–4 μM , which represented a maximum tetracycline concentration that was approximately $\frac{2}{3}$ of the aptamer concentration.

Using this information, a 7.2 μM aptamer solution was used to conduct all future experiments aimed at replicating the streptavidin studies, but this time using tetracycline. Again, a tetracycline standard curve was first obtained and is presented in **Figure 7**. The plot demonstrates a clear linear trend, with an R^2 value of 0.99. The variance observed for each point on the plot was significantly less than that observed for the streptavidin study, which is an indication of the variability in the pulsatile nature of the peristaltic pump. This curve was then used to analyze fluorescence readings from the tetracycline kinetic analysis experiment. Again, the raw data is provided in **Figure 8** and shows less fluctuation in the fluorescence signal. This data was again filtered and converted to the tetracycline concentration profile (**Figure 9**) using the standard curve. The results were again compared to an analytical model of the titration. The concentration rate of increase was measured as 245.5 nM/min, and integration of the signal resulted in a total

of determination was 0.99.

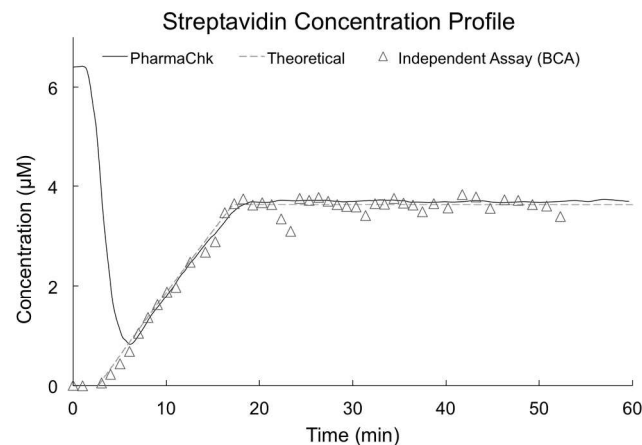


Figure 5 Streptavidin concentration profile using 18 μM B4F showing an increasing trend as streptavidin is titrated into the pill-dissolving vessel. Once the titrant has been consumed, the signal plateaus to a constant value. The initial decrease in concentration seen before the linear regions reflects the initial arrival of B4F to the microfluidic chip. Linear regime of microfluidic data shows an increase at a rate of 245.3 nM/min, as compared to 251.5 nM/min for the theoretical rate. Both the microfluidic data as well as the independent assay show close agreement with the theoretical profile.

API content of 46.8 μg . These values represented an error of 1.7% and 2.9%, respectively.

Discussion

The experimental results presented here demonstrate that a microfluidic, flow-through method can indeed be used to continuously monitor analyte concentrations. Furthermore, our work also demonstrates that aptamers can be used effectively as a reporter molecule to monitor drug concentration and drug dissolution at the point-of-care, currently a major problem in field-based drug testing. This may prove to be an incredible advantage due to the exceptional selectivity and thermostability that aptamers can offer over other specific binding molecules such as antibodies.

The streptavidin and tetracycline studies together provide a validation of the concept design as well as a demonstration of the use of this method to monitor a real drug. Both studies showed errors of less than 4% in quantifying analyte content and kinetic release, which represents a marked improvement over current, field-based technologies for counterfeit and substandard medicines detection. While the experiments demonstrated in this work were performed in a laboratory using bench-top equipment, prolific work is being conducted in the area of field-based fluorescence detection^{56–60} that can be used to rapidly translate this method into the field.

However, before this transition can occur, several technical challenges need to be addressed. The first is the effect of pulsatile flow on the fluorescence signal. The use of a peristaltic pump showed high variability in the pulsatile nature of the microfluidic flow, which was demonstrated by the difference in the error bars between the streptavidin and tetracycline standard curves. Video of the junction at the head of the SHM channel revealed the cause of the fluctuations to be out-of-phase pulsing of the analyte and reporter solutions

(Supplemental 2). This data showed that at the end of each pump cycle, there was brief backflow in one channel followed

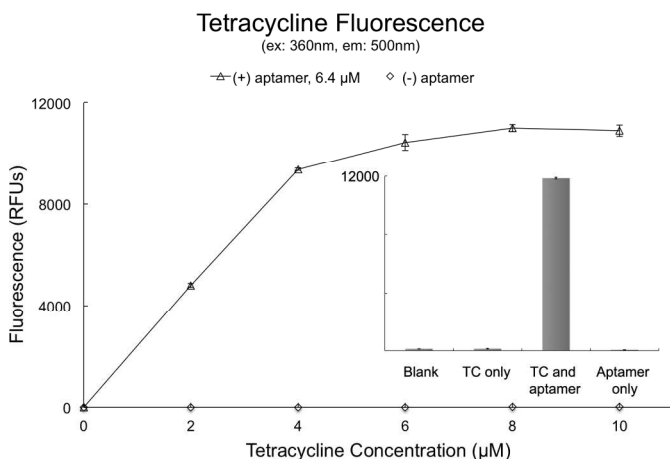


Figure 6 (inset) Tetracycline (10 μM) fluorescence measured with a spectrophotometer using an excitation wavelength of 360 nm and an emission wavelength of 500 nm. A blank and two controls demonstrate that a 90-fold increase in fluorescence is observed only when tetracycline and 6.4 μM aptamer are incubated together. (plot) Concentration curve of tetracycline fluorescence with and without the addition of 6.4 μM aptamer. Aptamer concentration was held constant for all samples regardless of tetracycline concentration. Plot shows a plateau region beginning at approximately 6 μM tetracycline, qualitatively demonstrating a 1:1 binding ratio of tetracycline aptamer to tetracycline.

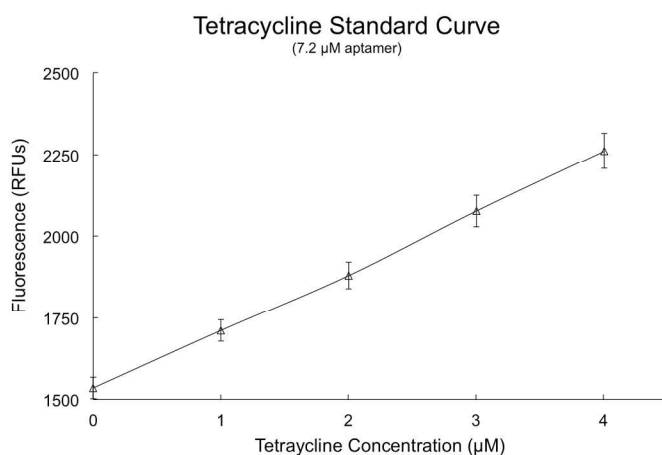


Figure 7 On-chip standard curve of tetracycline fluorescence obtained by flowing with a 7.2 μM aptamer reporter solution. Each point was obtained by averaging image frames captured at a rate of 2 Hz over 90s. Error bars are indicative of variations in signal caused by pulsatile flow in the system over this time period. The coefficient of determination was found to be 0.999.

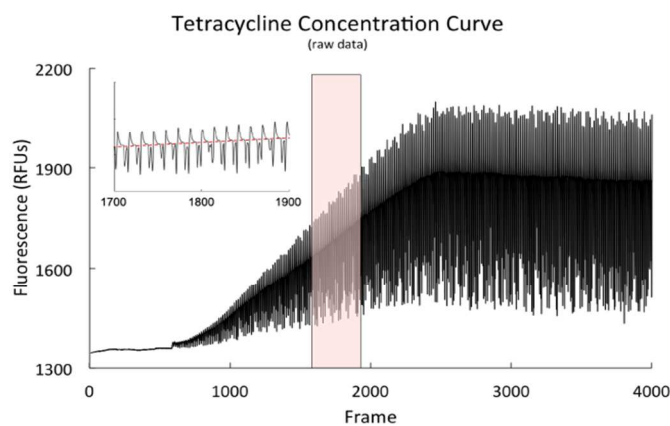


Figure 8 Plot of the raw tetracycline concentration curve, showing fluorescence against image frames during a simulated dissolution experiment. Again there are periodic fluorescence peaks and valleys that are due to the pulsatile nature of the peristaltic flow. The extent of the variations is smaller in comparison to the streptavidin data as fluorescence in this experiment is only observed when both tetracycline and the aptamer are mixed together in solution.

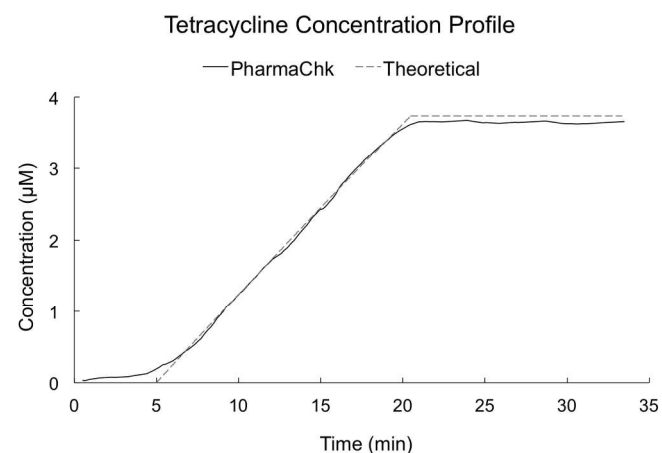


Figure 9 Tetracycline concentration profile showing a linear rate of increase as solubilized tetracycline is titrated into the dissolution apparatus at a constant rate. The signal plateaus to a final value of 3.65 μM once the titrant has been consumed. The rate of increase in the linear regime is 245.5 nM/min. Expected concentration profile based on computational model of the titration. Linear regime shows an increase of 241.5 nM/min and a plateau of 3.74 μM.

by a quick reversal with backflow into the other channel. This flow then stabilized again during the start of the next cycle, sending an appropriate mixture down the SHM channel. The downstream consequence of this behavior was a solution train during each pump cycle that was composed of mostly reporter, followed by mostly analyte, and then an appropriate mixture of

the two. In severe cases of the out-of-phase behavior, the train was composed of pure reporter, pure analyte, followed by the appropriate mixture (**Figure 10**).

A key contributing factor to these fluctuations may have been small variations in tubing diameter and length, which coupled with a high fluid resistance through the microfluidic

chip would result in brief backflows as the rollers of the peristaltic pump released one tube slightly before the other.

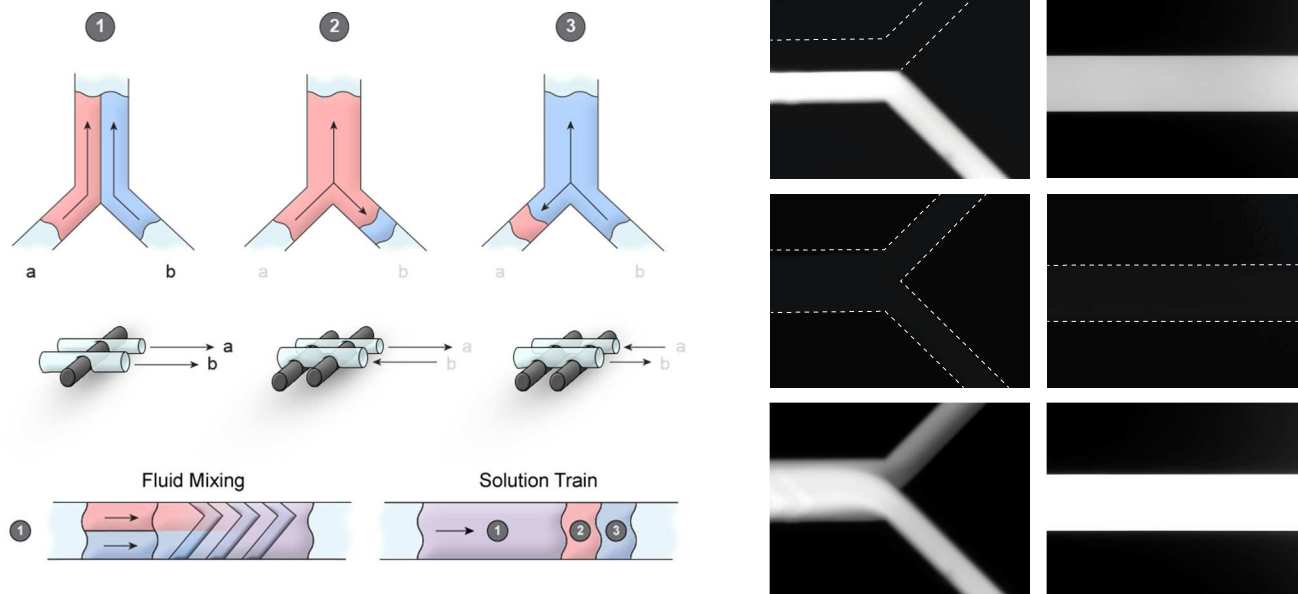


Figure 10 (left) Illustration of pulsatile flow effects on flow at the SHM channel junction. The beginning of each pump cycle sees a 1:1 ratio of both liquids converging and flowing down the SHM channel. Due to slight differences in tube diameter, the moving rollers of the peristaltic pump release from one tube before the other, cause backflow in that tube as pressure continues to drive fluid forward in the other tube. When the roller finally releases from the other tube, the larger pressure drop in this channel causes backflow in the reverse direction. As the subsequent roller pinches both tubes at the start of the next cycle, the fluids are again pushed down the SHM channel at 1:1 ratio. The downstream consequence of the fluid backflow is a solution train where the 1:1 mixture represents the relevant portion of the signal and composes the majority of the train, but small plugs of pure API and pure fluorescent tag are also present at the end of each pump cycle. In the streptavidin data, it is the pure API plug that is non-fluorescent and leads to the cyclic drop in signal whereas the pure fluorescent tag solution is fluorescent and leads to the cyclic spike in signal. (right) fluorescence images of experimental data depicting each of the three stages both at the SHM channel junction and downstream.

Compliance in the 1.02 mm ID tubing further stores energy during the pumping process as pressure builds to push fluid through the high-resistance microfluidic channels. While in the present study, an open pumping system was required in order to generate a dynamic analyte solution to simulate tablet dissolution, future work using real tablets could employ a closed pumping method such as a pressure-driven system. This would provide constant and continuous flow to the microfluidic chip, eliminating any fluorescence artifacts that may otherwise arise.

Conclusions

Counterfeit and substandard medicines are a grave public health concern that represents a serious and overlooked problem. While their initial emergence was seen largely in resource-limited areas of the world, they are quickly populating markets in more developed countries. In the United States alone, there has been over an 800% increase in the number of counterfeit medicines reported since 2000,⁶¹ many of which were for cancer drugs,⁶²⁻⁶⁴ and over the last 6 years there have been over 200 deaths related to poor quality medicines.^{7, 65}

While numerous technologies are available for medicines quality testing, none provide quantitative information regarding API content and kinetic release. Both of these attributes are critical factors for identifying poor quality medicines and are currently neglected in field-based screenings. Our results demonstrate an alternative approach to these existing methods

that is capable of specifically addressing this need. The approach presented here brings a new tool to the field for quantitative testing that can provide more reliable information regarding medicines quality. Our microfluidic platform promotes minimal resource usage, cutting costs and weight. Furthermore, our single chip design can be used to quantify any analyte, simply with the change of the reporter solution. While requiring the development of an extensive reporter library, this modular design permits organization of specific kits that can cater to the testing needs of different areas. Furthermore, improvements in detection can continue to be made through enhancements to the specificity and responses of the reporter molecules themselves. This allows for quick and easy deployment of next generation reporters that provide improved results without any changes to the detection hardware.

Our microfluidic approach presents an innovative, portable and affordable solution that addresses the technical needs absent in the field, while remaining conscious of the factors of field-based technologies that make or break their success. Although there are still many systems-level challenges that must be addressed to mitigate the distribution of substandard medication, our goal is to inch toward an exhaustive solution by specifically providing a targeted solution for medicines quality testing. Beside the existing array of medicines screening devices, this approach may help to provide an additional and more dependable safeguard against the adulterated medicines that continue to threaten the livelihood of millions around the world.

Acknowledgements

The authors acknowledge generous support from US Pharmacopeia Fellowship to Darash Desai and support from USAID's PQM Program and from Saving Lives at Birth. The authors would also like to acknowledge the work of Paul Vermillion for initial microfluidic chip validation and testing and Sonya Iverson for guidance in and troubleshooting of molecular biology protocols for aptamer expression and purification.

Notes and references

^a Department of Biomedical Engineering, Boston University. 44 Cummings Mall, Boston, MA 02215.

* Corresponding author: zaman@bu.edu

- J. Morris and P. Stevens, *Counterfeit medicines in less developed countries*, International Policy Network, London, 2006.
- M. Yasir, in *WeeklyPulse*, 2013.
- M. Forzley, *Combating Counterfeit Drugs: A Concept Paper for Effective International Cooperation*, World Health Organization, 2006.
- The Globalization of Crime: A Transnational Organized Crime Threat Assessment*, United Nations Office on Drugs and Crime, 2010.
- P. N. Newton, M. D. Green and F. M. Fernandez, *Trends in pharmacological sciences*, 2010, 31, 99-101.
- Lancet*, 2012, 379, 685-685.
- R. Bate, *Phake : the deadly world of falsified and substandard medicines*, AEI Press, Washington, D.C., 2012.
- The Economist*, 2010.
- M. Hajjou, Y. Qin, S. Bradby, D. Bempong and P. Lukulay, *Journal of pharmaceutical and biomedical analysis*, 2013, 74, 47-55.
- C. Ricci, L. Nyadong, F. Yang, F. M. Fernandez, C. D. Brown, P. N. Newton and S. G. Kazarian, *Analytica chimica acta*, 2008, 623, 178-186.
- R. Martino, M. Malet-Martino, V. Gilard and S. Balayssac, *Analytical and bioanalytical chemistry*, 2010, 398, 77-92.
- T. Puchert, D. Lochmann, J. C. Menezes and G. Reich, *Journal of pharmaceutical and biomedical analysis*, 2010, 51, 138-145.
- O. Rodionova, A. Pomerantsev, L. Houmoller, A. Shpak and O. Shpigun, *Analytical and bioanalytical chemistry*, 2010, DOI: 10.1007/s00216-010-3711-y.
- M. Tipke, S. Diallo, B. Coulibaly, D. Storzinger, T. Hoppe-Tichy, A. Sie and O. Muller, *Malaria journal*, 2008, 7.
- S. H. Scafi and C. Pasquini, *Analyst*, 2001, 126, 2218-2224.
- M. B. Lopes, J. C. Wolff, J. M. Bioucas-Dias and M. A. Figueiredo, *Analytical chemistry*, 2010, 82, 1462-1469.
- P. G. Risha, Z. Msuya, M. Clark, K. Johnson, M. Ndomondo-Sigonda and T. Layloff, *Health policy*, 2008, 87, 217-222.
- The International Pharmacopeia -- 4th ed.*, World Health Organization, 2013.
- R. Bate, R. Tren, K. Hess, L. Mooney and K. Porter, *African journal of pharmacy and pharmacology*, 2009, 3, 165-170.
- A. A. Weaver, H. Reiser, T. Barstis, M. Benvenuti, D. Ghosh, M. Hunckler, B. Joy, L. Koenig, K. Raddell and M. Lieberman, *Analytical chemistry*, 2013, 85, 6453-6460.
- V. P. Skipski, R. F. Peterson and M. Barclay, *Biochemical journal*, 1964, 90, 374-378.
- E. Marchand, M. A. Atemnkeng, S. Vanermen and J. Plazier-Vercammen, *Biomedical chromatography*, 2008, 22, 454-459.
- C. S. Gautam, A. Utreja and G. L. Singal, *Postgraduate medical journal*, 2009, 85, 251-256.
- A. Johnston and D. W. Holt, *British journal of clinical pharmacology*, 2013, DOI: 10.1111/bcp.12298.
- G. M. L. Nayyar, J. G. Bremen, P. N. Newton and J. Herrington, *Lancet infectious diseases*, 2012, 12, 506-506.
- C. Chrubasik and R. L. Jacobson, *Phytotherapy research*, 2010, 24, 1104-1106.

- P. Newton, S. Proux, M. Green, F. Smithuis, J. Rozendaal, S. Prakongpan, K. Chotivanich, M. Mayxay, S. Looreesuwan, J. Farrar, F. Nosten and N. J. White, *Lancet*, 2001, 357, 1948-1950.
- R. Miyake, T. S. J. Lammerink, M. Elwenspoek and J. H. J. Fluitman, *Proceedings of micro electro mechanical systems*, 1993, 248-253.
- J. Branebjerg, P. Gravesen, J. P. Krog and C. R. Nielsen, *Proceedings of the 9th annual international workshop on micro electro mechanical systems*, 1996, 441-446.
- F. G. Bessoth, A. J. deMello and A. Manz, *Analytical communications*, 1999, 36, 213-215.
- K. S. Drese, *Chemical engineering journal*, 2004, 101, 403-407.
- J. Cha, J. Kim, S. K. Ryu, J. Park, Y. Jeong, S. Park, S. Park, H. C. Kim and K. Chun, *Journal of micromechanics and microengineering*, 2006, 16, 1778-1782.
- S. Hardt, H. Pennemann and F. Schonfeld, *Microfluidics and nanofluidics*, 2006, 2, 237-248.
- S. W. Lee, D. S. Kim, S. S. Lee and T. H. Kwon, *Journal of micromechanics and microengineering*, 2006, 16, 1067-1072.
- R. H. Liu, M. A. Stremler, K. V. Sharp, M. G. Olsen, J. G. Santiago, R. J. Adrian, H. Aref and D. J. Beebe, *Journal of microelectromechanical systems*, 2000, 9, 190-197.
- V. Mengeaud, J. Jossierand and H. H. Girault, *Analytical chemistry*, 2002, 74, 4279-4286.
- H. Z. Wang, P. Iovenitti, E. Harvey and S. Masood, *Smart materials and structures*, 2002, 11, 662-667.
- Y. Lin, G. J. Gerfen, D. L. Rousseau and S. R. Yeh, *Analytical chemistry*, 2003, 75, 5381-5386.
- A. P. Sudarsan and V. M. Ugaz, *Lab on a chip*, 2006, 6, 74-82.
- J. T. Yang and K. W. Lin, *Journal of micromechanics and microengineering*, 2006, 16, 2439-2448.
- A. A. S. Bhagat, E. T. K. Peterson and I. Papautsky, *Journal of micromechanics and microengineering*, 2007, 17, 1017-1024.
- A. Asgar, S. Bhagat and I. Papautsky, *J Micromech Microeng*, 2008, 18.
- A. D. Stroock, S. K. W. Dertinger, A. Ajdari, I. Mezic, H. A. Stone and G. M. Whitesides, *Science*, 2002, 295, 647-651.
- A. D. Stroock, S. K. Dertinger, G. M. Whitesides and A. Ajdari, *Analytical chemistry*, 2002, 74, 5306-5312.
- P. B. Howell, D. R. Mott, S. Fertig, C. R. Kaplan, J. P. Golden, E. S. Oran and F. S. Ligler, *Lab on a chip*, 2005, 5, 524-530.
- J. T. Yang, W. F. Fang and K. Y. Tung, *Chemical engineering science*, 2008, 63, 1871-1881.
- C. M. Dundas, D. Demonte and S. Park, *Applied microbiology and biotechnology*, 2013, 97, 9343-9353.
- C. E. Chivers, E. Crozat, C. Chu, V. T. Moy, D. J. Sherratt and M. Howarth, *Nature methods*, 2010, 7, 391-393.
- A. Ebner, M. Marek, K. Kaiser, G. Kada, C. D. Hahn, B. Lackner and H. J. Gruber, *Methods Mol Biol*, 2008, 418, 73-88.
- M. J. Waner and D. P. Mascotti, *Journal of biochemical and biophysical methods*, 2008, 70, 873-877.
- G. Kada, H. Falk and H. J. Gruber, *Biochim Biophys Acta*, 1999, 1427, 33-43.
- G. Kada, K. Kaiser, H. Falk and H. J. Gruber, *Biochim Biophys Acta*, 1999, 1427, 44-48.
- C. Berens, A. Thain and R. Schroeder, *Bioorg Med Chem*, 2001, 9, 2549-2556.
- M. Muller, J. E. Weigand, O. Weichenrieder and B. Suess, *Nucleic Acids Res*, 2006, 34, 2607-2617.
- U. Forster, J. E. Weigand, P. Trojanowski, B. Suess and J. Wachtveitl, *Nucleic Acids Res*, 2012, 40, 1807-1817.
- T. Hanscheid, *Transactions of the royal society of tropical medicine and hygiene*, 2008, 102, 520-521.
- Y. Kostov, X. Ge, G. Rao and L. Tolosa, *Measurement science & technology*, 2014, 25, 025701.
- A. R. Miller, G. L. Davis, Z. M. Oden, M. R. Razavi, A. Fateh, M. Ghazanfari, F. Abdolrahimi, S. Poorazar, F. Sakhaie, R. J. Olsen, A. R. Bahrmand, M. C. Pierce, E. A. Graviss and R. Richards-Kortum, *PLoS one*, 2010, 5.
- J. Minion, H. Sohn and M. Pai, *Expert review of medical devices*, 2009, 6, 341-345.
- F. B. Myers, R. H. Henrikson, L. Y. Xu and L. P. Lee, *Proceedings of the 33rd Annual international conference of the IEEE engineering in medicine and biology society*, 2011, 3668-3671.
- Lancet*, 2008, 371, 1551.

- 1
2
3
4
5
6
7
8
9
10
11
12
13
14
15
16
17
18
19
20
21
22
23
24
25
26
27
28
29
30
31
32
33
34
35
36
37
38
39
40
41
42
43
44
45
46
47
48
49
50
51
52
53
54
55
56
57
58
59
60
62. *Another counterfeit cancer medicine found in U.S. - Illegal practice puts patients at risk*, U.S. Food and Drug Administration, 2012.
63. *Counterfeit Version of Avastin in U.S. Distribution*, U.S. Food and Drug Administration, 2012.
64. *Health Care Provider Alert: Another Counterfeit Cancer Medicine Found in United States*, U.S. Food and Drug Administration, 2013.
65. N. P. Keller, *Fungal genetics and biology*, 2013, 61, 142.